Formation of amyloid fibrils from ovalbumin under Ohmic heating

Eike Joeres [a,b], Stephan Drusch [b], Stefan Töpfl [c], Andreas Juadjur [a], Olympia Ekaterini Psathaki [d], Volker Heinz [a], Nino Terjung [a,*]

[a] *DIL – German Institute of Food Technologies (DIL e.V.), Professor-von-Klitzing-Str. 7, 49160, Quakenbrück, Germany*
[b] *Technical University of Berlin, Institute of Food Technology and Food Chemistry, Department of Food Technology and Food Material Science, Königin-Luise-Str. 22, 14195, Berlin, Germany*
[c] *University of Applied Science Osnabrück, Department of Agricultural Science and Landscape Architecture, Oldenburger Landstr. 62, 49090, Osnabrück, Germany*
[d] *University of Osnabrück, Department of Biology/ Chemistry, Barbarastr. 11, 49076, Osnabrück, Germany*

A B S T R A C T

Ohmic heating (OH) is an alternative sustainable heating technology that has demonstrated its potential to modify protein structures and aggregates. Furthermore, certain protein aggregates, namely amyloid fibrils (AF), are associated with an enhanced protein functionality, such as gelation. This study evaluates how Ohmic heating (OH) influences the formation of AF structures from ovalbumin source under two electric field strength levels, 8.5 to 10.5 and 24.0–31.0 V/cm, respectively. Hence, AF aggregate formation was assessed over holding times ranging from 30 to 1200 sunder various environmental conditions (3.45 and 67.95 mM NaCl, 80, 85 and 90 °C, pH = 7). AF were formed under all conditions. SDS-PAGE revealed that OH had a higher tendency to preserve native ovalbumin molecules. Furthermore, Congo Red and Thioflavin T stainings indicated that OH reduces the amount of AF structures. This finding was supported by FTIR measurements, which showed OH samples to contain lower amounts of beta-sheets. Field flow fractioning revealed smaller-sized aggregates or aggregate clusters occurred after OH treatment. In contrast, prolonged holding time or higher treatment temperatures increased ThT fluorescence, beta-sheet structures and aggregate as well as cluster sizes. Ionic strength was found to dominate the effects of electric field strength under different environmental conditions.

1. Introduction

While conventional heating (COV) processes in food production are commonly based on conduction, convection or radiation [1], Ohmic heating (OH, also known as Joule heating or resistance heating) is a volumetric heating technology, in which a food is placed between two electrodes and an electrical current is run through the food [2]. The food itself acts as an electrical resistor, resulting in the conversion of electrical energy into thermal energy within the food product [2]. Electrical field strengths applied during OH are commonly around 0–1000 V/cm and are considered as moderate electric fields (MEF) [3]. Compared to COV processes, OH provides a more homogenous heating and higher energy conversions. Therefore, OH is a more sustainable heating technology, as the process does not require any fossil energy sources but only electrical energy to be run [4]. Furthermore, OH has also shown its potential to be used as a tool to tailor the functionality of certain food ingredients, e.g., proteins [5].

---

* Corresponding author.
  E-mail address: n.terjung@dil-tec.de (N. Terjung).

During heat processes in food production, thermal energy can induce molecular and structural changes in proteins [6,7]. Many food proteins can be categorized as globular proteins, exhibiting a well-defined secondary and tertiary protein structure, like ovalbumin or β-lactoglobulin [8]. Upon heating above their denaturation temperature, globular proteins typically unfold their spherical molecule structure and subsequently form aggregates and/or gel network structures [9]. The specific environmental conditions during heating (e.g., pH, ionic strength, or treatment time play a crucial role in determining the aggregation patterns, resulting in aggregates of varying sizes and shapes. It includes the formation fibrillar or spherical aggregate structures [8,10]. In the case of ovalbumin, thermal aggregation under neutral pH has been described to produce fibrillar or rod-shaped aggregates at low ionic strength. At high ionic strength, these fibrillar or rod-shaped aggregates assemble into branched clusters [11,12].

Fibril protein structures like amyloid fibrils (AF) gained importance in food science over the last decades, as they have shown to enhance protein functionality and can be used to tailor several food properties. This includes augmenting the stability of emulsions or foams, as AF can create viscoelastic interfaces between the phases that a more robust and exhibit a higher aspect ratio than native proteins [13]. Given that AF also possess a high chemical resistance and mechanical strength, these protein structures have exhibited potential to be used as building blocks for food gels, having positive impacts on gel strength, gel structure or viscosity [14,15].

Currently, the formation of AF is described as a generic property of proteins, arising when proteins lose their native state [10,16]. In food science, AF formation is typically induced under the influence of heat treatment and acidic conditions, as this environment allows denaturation as well as partially hydrolysis of the native proteins, which is described to precede AF formation. However, several studies have also described AF formation under heat treatment at neutral pH conditions, as also reviewed in literature [17] At a molecular level, AF are insoluble fibrillar protein structures of nanometre scale, typically arising as a consequence of protein aggregation [18]. During AF formation, aggregation-prone regions of the proteins assemble into highly ordered cross-beta core structures, which elongate from oligomers to protofilaments and finally into mature AF [18].

Proteins or protein aggregates have been described to be affected by non-thermal effects of MEF during OH [19]. These effects are also related to interactions of the MEF with loaded areas of proteins, which cause motions of the molecules. Samaranayake & Sastry [20] describe translational as well as rotational motions of α-amylase molecules caused by MEF, whereas motions varied from oscillating behaviour to full rotations at low or high electrical frequencies, respectively. Within the last years, several studies have reported non-thermal effects during OH on denaturation and aggregation of several proteins from different sources like whey, egg white, legumes, oil seeds or tubers. These non-thermal effects are described to lead to less denaturation but more soluble proteins, formation of smaller aggregates, deviations in the formation of molecular bonds and/or interactions as well as differences in surface hydrophobicity of aggregates when compared to COV [3,21–24]. Furthermore, the influence of an altered conformation on protein functionality as well as the influence of MEF on microbiological inactivation is part of published research [21,25,26].

Information about the influence of MEF on the formation of AF is limited. Pereira et al. [27] investigated whey protein aggregation under OH at pH 3 and reported enhanced fibril-resembling protein aggregates when heated via OH compared to COV. Joeres et al. [25] studied the influence of MEF on aggregation, gelation and gel properties of egg white protein. Thereby, OH treated samples showed lower mechanical strength as well as lower beta-sheet structures, which could be indicative for lower AF structures when MEF are applied.

Noteworthy, several studies were conducted evaluating the influence of electric fields on AF at higher field strengths, i.e., pulsed electric fields (PEF), or under electromagnetic waves (i.e., microwaves). In contrast to MEF, PEF are applied at field strengths of approx. 0,5–100 kV/cm and typically for very short time intervals, leading to no or just little heat generation [3]. Jurgelevičiūtė et al. [28] describe PEF treatment of AF originating from yeast leading to reductions of fibril length as well as a disintegrational effect on fibril structures. Comparable effects of PEF on AF (e.g., from human serum albumin) are also reported by other authors [29]. Microwave treatment has shown partially contrary behaviour. Hettiarachchi et al. [30] and Todorova et al. [31] describe both inhibiting as well as enhancing effects of the electromagnetic waves on AF formation (e.g., from beta-lactoglobulin source).

To fill the scientific gap on the influence of MEF on the formation of amyloid fibrils from food proteins, this study was set up. To the best of our knowledge this is the first time the formation of amyloid fibrils under MEF is evaluated. Ovalbumin was chosen as model protein as it has shown its potential to develop AF structures under various environmental conditions [32,33]. Based on literature, our hypotheses states, that non-thermal effects and MEF-induced motions during OH will lead to less intermolecular interactions via cross-beta sheet structures, resulting in less or smaller sized AF aggregates compared to COV. Further we expect that longer heating times and higher temperatures increase the formation AF structures during both heating methods, OH and COV. To check our hypothesis, three temperatures near the denaturation temperature of ovalbumin were defined, at which AF formation is evaluated: 80, 85 and 90 °C. Two holding times (HOLD) were established to survey AF formation over treatment time of 20 min. To study changes in the electric field strength during OH as well as the appearance of ovalbumin aggregates, two ionic strengths were used. As a primary criterion for the formation of AF, Congo Red (CR) staining was performed. Thioflavin T (ThT) staining was applied to monitor AF formation over HOLD and field flow fractioning (FFF) revealed information about shifts in aggregate sizes. Optical information about size and shape of AF were established using transmission electron microscopy (TEM). Additionally, changes in secondary protein structures within the treated samples were studied via Fourier-transform infrared spectroscopy (FTIR).

2. Materials and methods

2.1. Protein solution preparation

Ovalbumin with a purity of ≥98 % (agarose gel electrophoresis) was bought from Sigma-Aldrich (Sigma-Aldrich Corporation, St. Louis, USA). All used salts for preparing buffer solutions as described below are of analytical grade. Two buffers at pH 7 were used for

preparing the protein solutions, which are called "low" and "high" in the further text, as these buffers contained low or high ionic strength. The pH was measured at room temperature using a FiveGo pH meter F2 by Mettler Toledo (Mettler Toledo Inc., Columbus USA). Both buffers were made from Mili-Q water and had following further ingredients: 5.00 mM NaH_2PO_4 and 0.01 wt% NaN_3. Buffer with low ionic strength additionally contained 3.45 mM NaCl and buffer with high ionic strength container 67.95 mM NaCl. Latter is the NaCl content of native egg white protein, which had already been described elsewhere [25]. The low ionic strength buffers NaCl content results from the adjustment of NaCl to the here used protein concentration compared to native egg white protein, which was 0.50 wt%. Solutions were prepared by adding the protein to the respective buffer and gentle stirring for 2 h at room temperature. Afterwards protein solutions were stored overnight at 4 °C to allow full hydration. After 16 h of hydration, protein samples were again gently stirred for 30 min to allow temperature equilibration to room temperature. Before starting of heat treatment, samples were brought to a common starting temperature of 25 °C.

2.2. Heat treatment

COV was performed using aliquots of 1200 μl in 1500 μl screw caps. Heating was done in a laboratory block heater, which was set to a fixed temperature of 93 °C. After reaching the final temperatures of 80, 85 or 90 °C, samples were taken after 30/300/600/900 and 1200 s. Samples which were taken after 30 s are further described as "short HOLD" and samples taken after 1200 s are referred to as "long HOLD". Identical thermal treatments to the COV counterparts were performed via OH. Therefore, the electric field strength was manually adjusted. For OH samples, 40 ml of protein solution was heated in an Ohmic heating cell, which consists of 20.0 mm thick sidewalls and bottom made of polyethylene and 0.5 mm thick electrodes made from stainless steel. The gap between electrodes is 200 mm and 10 mm between sidewalls. The cells lid is made from 10 mm thick polyethylene. Temperature measurement was done using a PT-100 thermocouple (type HET/E, FuehlerSysteme eNet International GmbH, Nürnberg, Germany), positioned in the centre of the solution. Electrical function generator used is a pilot plant from the German Institute of Food Technologies (DIL e.V.) as described elsewhere [25]. A schematic diagram as well as a picture of the experimental OH set-up utilized can be found in the supplementary material.

2.3. Aggregate analysis

2.3.1. SDS-PAGE

An SDS-PAGE was performed using the heated samples as well as unheated control samples at 0.5 wt% protein concentration in respective buffers with high or low ionic strength. The SDS-PAGE run was performed as described by Joeres et al. [25], whereby protein solutions were mixed with 400 μl Laemmli buffer and heated at 100 °C for 10 min. Centrifugation was performed for 10 min at 15,000 rpm before loading samples onto a 4–20 % Criterion™ TGX™ Precast Midi Protein Gel (Biorad Laboratories Inc., Hercules, USA). Electrophoresis was run at 200 V for 45 min and Sigma Marker™ Wide Range 6, 6.500–20.000 Da (Sigma Aldrich, St. Louis, USA) was used as a molecular marker.

2.3.2. Congo red staining

CR staining was done as described by Josefsson et al. [34] with slight modifications. Therefore, a CR stock solution was prepared by dissolving 3.5 mg CR in 1 ml PBS buffer (pH 7) and subsequently filtered through 0.2 μl syringe filter membrane. Working solution was prepared by diluting 5 μl of stock solution in 955 μl PBS buffer. The 980 μl working solution was placed in a plastic cuvette (1 cm path length), 20 μl of sample were added and incubated for 30 min before measuring absorbance with a Specord 40 UV/VIS spectropho-tometer (Analytik Jena GmbH, Jena, Germany) between 400 and 600 nm.

2.3.3. Thioflavin T staining

According to Monge-Morera et al. [16] ThT staining was performed. Samples were diluted to 0.1 wt% using ThT buffer (50 mM NaH_2PO_4, 0.01 wt% NaN_3, pH 7) and 190 μl sample were placed in respective wells in a flat black 96-well plate chimney (Greiner Bio-One GmbH, Frickenhausen, Germany). ThT was dissolved to a concentration of 200 μm in ThT buffer under stirring and subse-quently filtered through 0.2 μm syringe filter membrane. 10 μl of ThT solution was added to each well and fluorescence was imme-diately measured at excitation and emission wavelength of 440 and 481 nm, respectively.

2.3.4. Field flow fractioning

Before FFF runs, samples were diluted to a protein concentration of 0.1 wt%, filtered through a 0.1 μm membrane and ThT was added as described in section 2.3.2. 20.0 μl of sample were injected per run and fractioned over an Eclipse long channel poly-ethersulfone membrane (Wyatt Technology Corpporation, Santa Barbara, CA, USA) with a 10 nm cut-off. 50 mM NaH_2PO_4 buffer filtered through 0.1 μm membrane was used as FFF buffer. Inject flow, channel flow and detector flows were kept constant throughout FFF at 0.2, 1.0 and 0.5 ml/min, respectively. Fractioning was performed using the following cross flow steps: An initial focussing step at 0.0 ml/min was applied for approx. 10.0 min. Subsequently, 5.0 min were run at 3.25 ml/min cross flow, followed by a second fractioning step, whereby cross flow rate was exponentially decreased from 3.25 to 0.05 ml/min over a time of 19 min. FFF was performed using the Wyatt Eclipse™ system in combination with a Wyatt multi-angle light scattering detector DAWN®. UV mea-surements at 280 nm were conducted using an Agilent 1260 Infinity II Variable Wavelength Detector and ThT fluorescence was measured via Agilent 1260 Infinity II fluorescence detector (Agilent Technologies Inc., Santa Clara, CA, USA). Wyatt software Vision Design™ and Vision Run™ was used performing FFF and Wyatt software Astra (Wyatt Technology Corporation, Santa Barbara, CA,

USA) was used for further analysis.

2.3.5. Transmission electron microscopy

TEM imaging was performed as proposed by Monge-Morera et al. [16] with slight modifications. Therefore, samples were diluted 1:20 with Mili-Q water and 5 µl of sample was placed on a glow discharged copper grid. After washing with Mili-Q, negative staining was done using 2 wt% uranylacetate for 60 s, followed by another washing step with Mili-Q water. Images were taken at from dried grids using a ZEISS TEM LEO 912 (Carl Zeiss AG, Oberkochen, Germany).

2.3.6. Fourier-transform infrared spectroscopy

FTIR measurements were done as described elsewhere [35], using undiluted protein samples of 0.5 wt% protein content. A Bruker Tensor II spectrometer (Bruker Optik GmbH, Karlsruhe, Germany) with a ATR transmission cell (Bio-ATR II multiDTC by Bruker Optik, Karlsruhe, Germany), whereas the spectrometer comes with a nitrogen cooled mercury-cadmium-telluride detector. A resolution of 4 cm^{-1} at 120 scans within an wavenumber range of 1000–3000 cm^{-1} were used for taking FTIR spectra. Demineralised water was used a blank. Second derivate was done in the wavenumber range of 1470–1720 cm-^{1} and all spectra were normalised and smoothed using the 25-point-Savitsky-Golay-method. Numeric approximations of the respective second derivative spectra were performed to quantify the relative amount of intermolecular beta-sheet structures. OPUS 5.7 by Bruker Optik GmbH was software used (Karlsruhe, Germany).

2.3.7. Statistical analysis

All samples were prepared in triplicate execution for each buffer. When possible, two or more technical duplicates were taken for data collection. Independent variables used were time, temperature, and ionic strength as well as heating methods, i.e., OH and COV. Dependent variables were e.g., the amount of respective secondary protein structure. To conduct statistical analysis, Sigma Plot 13 (Systat Software Inc., San Jose, California, USA) was used by performing ANOVA followed by Tukey or Holm-Sidak postHoc test. Standard deviations are expressed as error bars in plots or given in tables. Significant statistical differences with a significance level of $P < 0,05$ are indicated via superscripts.

3. Results and discussion

Preparation of protein solutions with high or low ionic strength resulted in different electrical conductivities, due to an increased salt content. Consequently, protein solutions with high ionic strength required treatment with lower electric field strengths, while those with low ionic strength necessitated higher field strengths, all to maintain consistent treatment durations. Electrical conductivities as well as treatment time and resulting electrical parameters during OH are shown in Table 1.

3.1. SDS-PAGE

To assess whether some ovalbumin monomers remain soluble during heat treatment, SDS-PAGE was conducted. Results from SDS-PAGE showed that ovalbumin band intensities decreased with increasing final temperature and elongation of HOLD as shown in Fig. 1 (a, b). This result is in line with results from literature as a higher energy input due to higher temperature or longer HOLD promotes protein denaturation and aggregation. This augmented energy, in addition to heating effect, leads to a greater number of proteins losing their solubility [36,37].

Results from SDS-PAGE showed that at low temperature and short heating time (i.e., at 80 °C and after short HOLD) more ovalbumin remained in a soluble form when heated via OH than under COV, as shown in Fig. 1 (a, b). Similar findings have been reported by other authors (e.g., for egg white protein, whey protein or potato protein) who propose that altered conformations or oscillating vibrations hinder the participation of protein molecules in aggregates or gel network structures, allowing them to maintain in a (partially) native form [21,22,25]. This phenomenon was visible at short HOLD as well as for low and high ionic strength at a final temperature of 80 °C. However, as proteins solutions were heated to temperatures above denaturation temperature of ovalbumin (85 and 90 °C) this distinction became less pronounced or entirely disappeared as both heating methods showed comparable band intensities for ovalbumin under both salt and HOLD conditions.

Table 1
Electrical and time parameters measured during Ohmic heating runs for ovalbumin solutions (0,5 wt%, pH 7) at different ionic strengths as indicated.

|	Electrical conductivity at 25 °C	Electrical parameters during come-up time		Electrical parameters during holding time		Come-up time to final temperature			Holding time
	(mS/cm)	EF strength (V/cm)	Current (A)	EF strength (V/cm)	Current (A)	to 80 °C (sec)	to 85 °C (sec)	to 90 °C (sec)	(sec)
Low ionic strength (3,45 mM NaCl)	0.85 ± 0.04	24.0–31.0	0.07–0.12	23.0–24.5	0.08–0.10	810 ± 15	930 ± 10	1170 ± 10	30 to 1200
High ionic strength (67,95 mM NaCl)	6.82 ± 0.02	8.5–10.5	0.12–0.31	7.0–7.5	0.12–0.14	810 ± 15	930 ± 10	1170 ± 10	30 to 1200
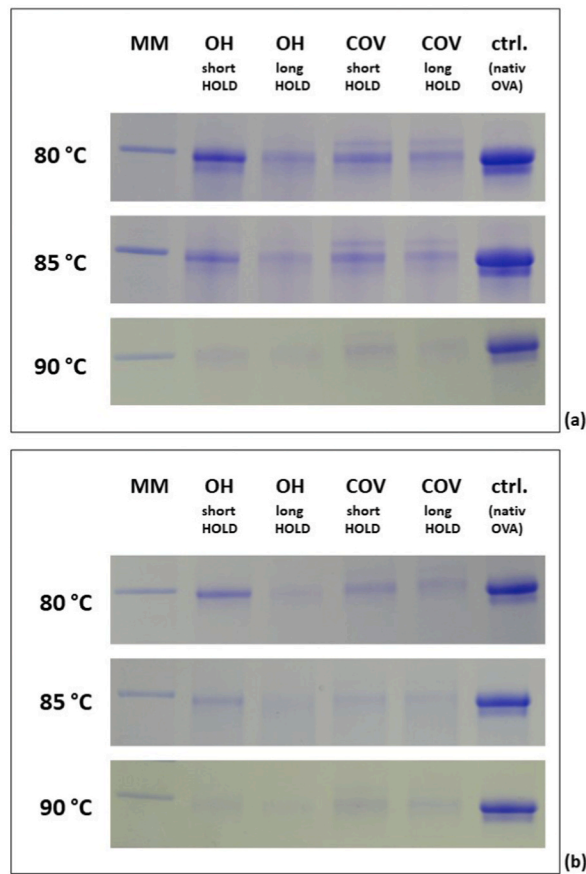
Fig. 1. SDS-PAGE results showing the ovalbumin band at approx. 40 kDa at various temperatures, holding times (HOLD), heating methods (OH = Ohmic heating, COV = conventional heating) and ionic strength: (a) at low ionic strength and (b) at high ionic strength. MM = molecular marker, ctrl. = untreated ovalbumin.
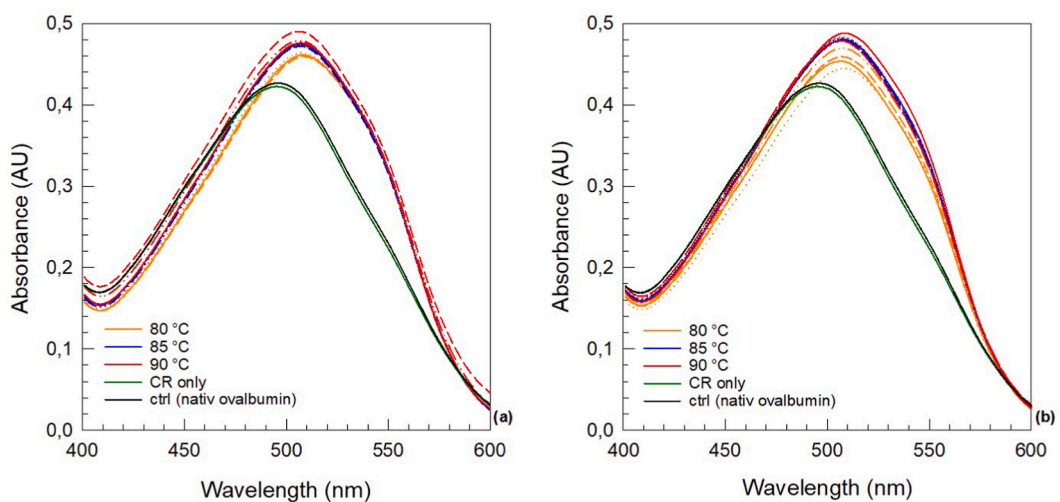

Fig. 2. Congo Red (CR) spectral shift assay results for 0,5 wt% ovalbumin solutions at pH 7 heated at various temperatures, holding times, heating methods and ionic strengths: (a) at low ionic strength, and (b) at high ionic strength. Straight lines: Ohmic heating (OH) at short HOLD, dotted lines: conventional heating (COV) at short HOLD, dashed lines: OH at long HOLD, dotted and dashed lines: COV at long HOLD. Temperatures are indicated via colors as shown.

3.2. Congo red staining

CR staining served as a primary criterion for identifying AF [38]. A higher absorbance indicates an augmented interaction between CR molecules and AF structures [39,40]. During a CR spectral shift assay, staining of AF with CR leads to a red shift in the absorbance from approx. 490 towards 520 nm [41]. Our results show this red shift for all heat-treated samples, indicating the formation of AF structures under all conditions used (see Fig. 2 (a, b)). In contrast, untreated ovalbumin does not show any spectral shift upon staining with CR. This initial observation suggests that AF formation from ovalbumin was achieved via both heating methods at temperatures from 80 to 90 °C.

Additionally, within the obtained results, a distinct trend emerged: CR absorbance was notably higher for samples heated at 85 and 90 °C than at 80 °C. In agreement with our results from SDS-PAGE (section 2.3.1), a higher thermal energy input into the system leads to higher levels of ovalbumin denaturation, as more energy is also available for denaturation of ovalbumin besides the overall heating of the system [42]. An increased denaturation of protein molecules fosters increased aggregation, which is a fundamental step for AF formation [17]. Hence, an increased AF formation resulting from more denaturation and aggregation because of higher energy input is likely to occur.

3.3. Thioflavin T staining

To gain deeper insights in AF formation during HOLD after reaching the final temperatures, ThT staining was conducted. ThT is renowned for its affinity to bind at cross-beta sheet structures, rendering it a dependable indicator for AF formation [38,40]. Noteworthy, ThT fluorescence signal can also be influenced by native proteins.

The results of the ThT staining are shown in Fig. 3. When examining the formation of AF during HOLD at various final temperatures, ionic strengths and the two heating methods, three main observations emerged:

  i) With an increase of temperature and/or HOLD, ThT fluorescence increases,
 ii) Samples objected to OH exhibited lower ThT fluorescence values than their COV counterparts,
iii) samples at low ionic strength displayed different ThT fluorescence pattern over HOLD when compared to samples at high ionic strength.

Observation i) is in line with results drawn from SDS-PAGE and CR, i.e., a higher or longer thermal treatment leads to more ThT fluorescence. This indicates a greater occurrence of AF structures in these samples. Similar findings are also described by Pearce et al. [33]. The most likely reason (higher energy input, thus, more denaturation) for this phenomenon has already been described in section 2.3.2.

Regarding observation ii), the results indicate that samples treated with OH present a lower amount of AF structures. Since ThT content remains equal in all samples, the variance in ThT fluorescence is associated with the quantity of AF structures [43]. Lower amounts of AF structures are possibly due to less or smaller-sized AF, resulting in an overall lower AF content within the sample. Given that both heating methods underwent equivalent thermal treatments, non-thermal effects are likely to either impair the formation of AF structures or having a disruptive impact on already built AF structures during OH. Pandey et al. [29] describe a disruptive influence
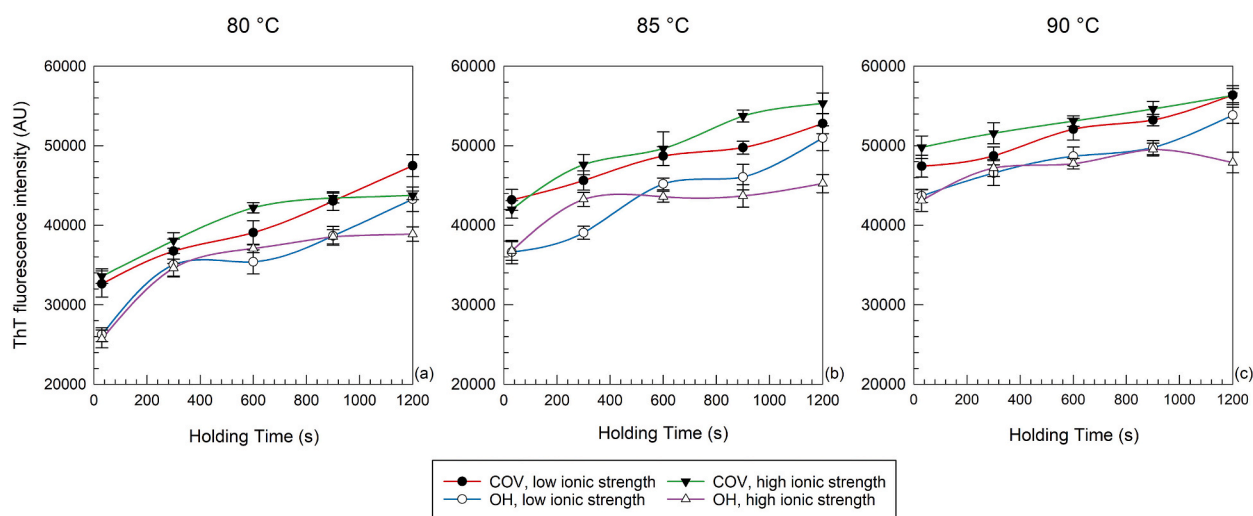

Fig. 3. Thioflavon T (ThT) staining results of 0,5 wt% ovalbumin solutions at pH 7 heated over 1200 s holding time via Ohmic heating (OH) and conventional heating (COV) and ionic strengths as indicated. Heating temperatures are (a) 80 °C, (b) 85 °C, and (c) 90 °C. Untreated ovalbumin solutions showed ThT fluorescence intensity values of approx. 3600–4400 AU.

of an electric field onto AF under PEF treatment. However, in our case, the electric field strength utilized is approx. 100-fold lower, making a disruptive behaviour far less likely under MEF than under PEF. Moreover, since the formation of mature AF starts within the heating time, the number of mature fibrils will be low. Consequently, we ascribe lower ThT fluorescence of OH samples to non-thermal effects of the MEF. Hence, non-thermal effects partially inhibit the formation of AF structures.

When looking at observation iii), samples heated at high ionic strength show an increase of ThT fluorescence the first half of HOLD and then reaching a plateau (except COV at 90 °C). This plateau starts earlier for OH samples, whereas at 90 °C, there is no plateau visible but a constant linear increase over HOLD. Monitoring the ThT fluorescence of samples at low ionic strength, final values of ThT fluorescence of OH and COV samples after long HOLD are close. In contrast, at high ionic strength, the ThT values after long HOLD differ more between OH and COV in comparison to short HOLD. This indicates that disparities between OH and COV decrease over HOLD when heated at low ionic strength but increase when heated at high ionic strength. This observation suggests that MEF hinder the formation of AF structures when heated at high ionic strength compared to low ionic strength. This result was unexpected, especially as samples at low ionic strength were subjected to stronger electric fields. Rodrigues et al. [44] describe higher electric field strength and lower frequencies to potentiate MEF effects. However, our results indicate the ionic strength to dominate the formation of AF structures over the influence of the electric field at the electrical set-up utilized. Therefore, it appears that environmental conditions during heating have a more pronounced impact on AF formation than the non-thermal effects of MEF.

3.4. Field flow fractioning

As shown in Fig. 4, three detectors were employed for the analysis of ovalbumin aggregates subsequent after sample fractionation. A light scattering (LS) detector provides information about the overall size of aggregates or aggregate clusters. An ultraviolet light (UV) monitored the UV absorbance of soluble proteins and aggregates at 280 nm. Furthermore, fluorescence (FL) detection revealed where ThT staining has occurred within the aggregates, indicating the presence of AF structures. Within the obtained results, three major peaks were identified within treated and/or control samples (as indicated in Fig. 4 (c)). Peak 1 appears after a retention time of approx. 11 min and corresponds to native ovalbumin, which is not yet denatured. This peak is clearly visible and represents the most dominant peak within control samples, which have not undergone any heating. Peak 2 emerges at a retention time of ca. 16 min and is attributed to ovalbumin aggregates. Similar fibrillar or rod/worm-like shaped aggregates have been reported by other authors and they are characteristic of ovalbumin aggregates under the environmental conditions utilized in this study [12,16]. Peak 3 reaches its maximum after a retention time of approx. 23 min and is linked to larger sized aggregate clusters. Aggregates of ovalbumin under comparable environmental conditions are described as branched clusters from fibrillar aggregates, whereas the degree of clustering is associated
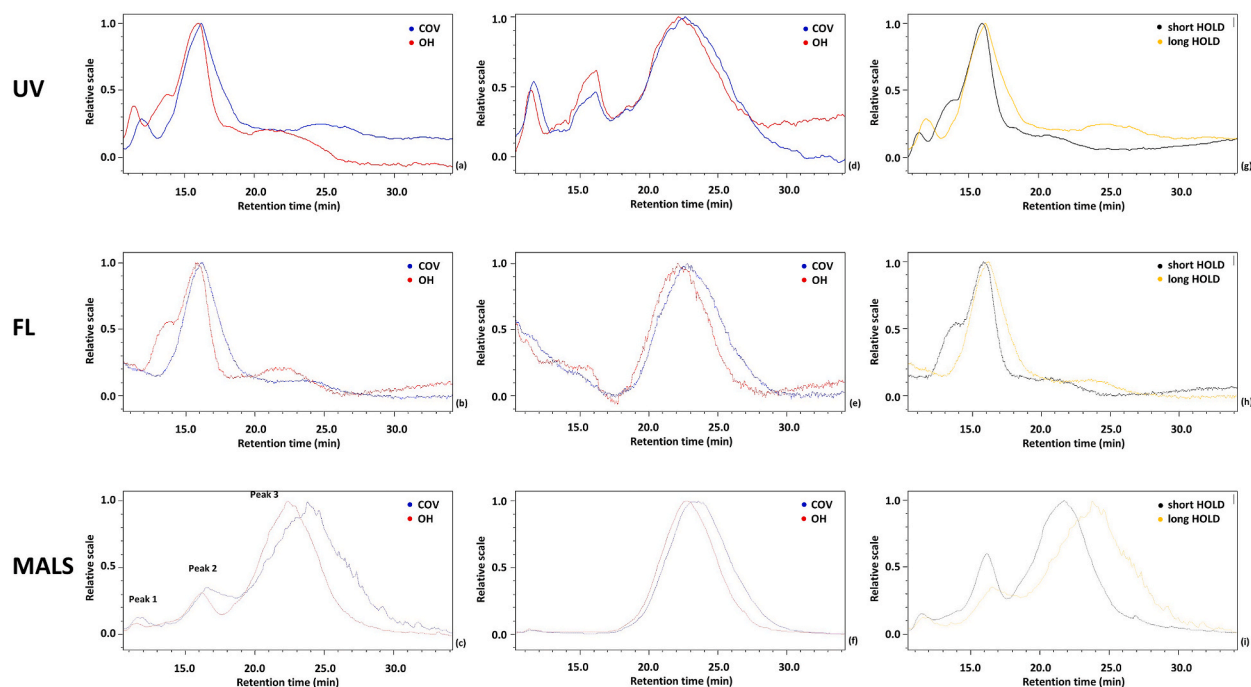

Fig. 4. Representative field flow fractioning chromatographs of heated of 0,5 wt% ovalbumin at pH 7 and 85 °C via Ohmic or conventional heating (OH, COV). Protein solutions heated at low ionic strength and high ionic strength are shown in (a), (b), (c), and (d), (e), (f), respectively, via different heating methods as indicated. Proteins solutions heated at low ionic strength for various holding times (HOLD) as indicated are shown in (g), (h) and (i). UV = ultraviolet light detector, FL = fluorescence detector (in combination with Thioflavin T staining), MALS = Multi angle light scattering detector.

with a reduction in repulsive forces [12]. These clusters arise, due to diminished repulsive forces between ovalbumin aggregates. Thus, peak 2 gives more information about the general size of single fibrillar shaped ovalbumin aggregates whereas the size of clusters can be deduced from peak 3.

In general, we observed a sharp decrease of UV signal from peak 1, but an increase in peak 2 and/or peak 3 in all treated samples compared to untreated control samples (data not shown). At treated samples, peak 2 becomes hardly or not at all visible under high ionic strength conditions (as shown in Fig. 4 (d)–(f)), indicating diminished repulsive forces between proteins and aggregates. Hence, primarily clusters of ovalbumin aggregates form under high ionic strength, aligning with existing literature [45]. ThT fluorescence signal also dominates in peak 3 under high ionic strength conditions, indicating a prevalent involvement of AF structures in these clusters. However, under low ionic strength, the ThT fluorescence signal is mainly visible in peak 2, with partial light fluorescence occurring in peak 3 partially (as shown in Fig. 4 (a)–(c)). Pearce et al. [33] also describe the impact of ionic strength on AF formation of ovalbumin to be less relevant compared to treatment temperature, which aligns with our results from CR staining. Nonetheless, based on our FFF results, we state that ionic strength plays a major role on the occurrence of AF structures. Specifically, it determines whether AF structures exist as linear single aggregates or as part of branched aggregate clusters. Examining our ThT staining results (as described in section 2.3.2), it is apparent that at high ionic strength, AF structures tend to reach plateau after certain treatment time. This suggests that aggregate clusters of ovalbumin might hamper further AF growth.

When comparing FFF results of samples treated at different temperatures or HOLD, a noticeable trend emerges towards longer retention time for peak 2 and/or peak 3. This indicates an increase in aggregate size and aggregate cluster size, with higher temperatures or prolonged HOLD (as shown in Fig. 4 (g)–(i)). Koseki et al. [46] also describe larger ovalbumin aggregates with greater energy input, which is in line with our findings.

When examining the impact of OH on peak occurrence in comparison to the corresponding COV treated samples, there is also a shift in retention time. Here, peak 2 and more notably peak 3 of OH treated samples emerge after less retention time, signifying smaller aggregates and aggregate clusters. This shift is particularly evident at 85 °C compared to 80 and 90 °C, indicating that the influence of MEF on aggregate size is less pronounced below denaturation temperature and diminishes further beyond it. Comparable findings are reported by several authors for whey proteins [23,27,44,47]. Furthermore, Rodrigues et al. [19] report synergistic effects of MEF with thermal unfolding of whey proteins, while Pereira et al. [22] describe MEF effects to become less when HOLD is prolonged. Our results on ovalbumin align with these effects, indicating a comparable influence on the shift in aggregate or cluster size, which is more pronounced at 85 °C.

In addition to the shift in retention time, also a distinction in peak shape of ThT fluorescence was evident between OH and COV treated samples at low ionic strength. Samples treated at low ionic strength under OH exhibit a shoulder at the beginning of peak 2, approx. after 12–14 min. This shoulder is less pronounced or entirely absent when samples were treated via COV (see Fig. 4 (b)). This further contributes to the finding, that aggregates showing AF structures are smaller in size when treated via OH.

3.5. Transmission electron microscopy

TEM micrographs support findings from FFF as no aggregate clusters could be observed within samples produced under low ionic strength. Under these conditions, fibrillar-shaped aggregates were discernible for all temperatures, HOLD and both heating methods. This aligns with Koseki et al. [46], who describe that ovalbumin aggregation at pH 7, at or above temperatures of 80 °C, leads to linear polymers but less monomers. This correlation supports the obtained results, as all samples show comparable visible aggregate structures at low ionic strength (as shown in Fig. 5 (a)). Micrographs from samples heated at high ionic strength exhibited the
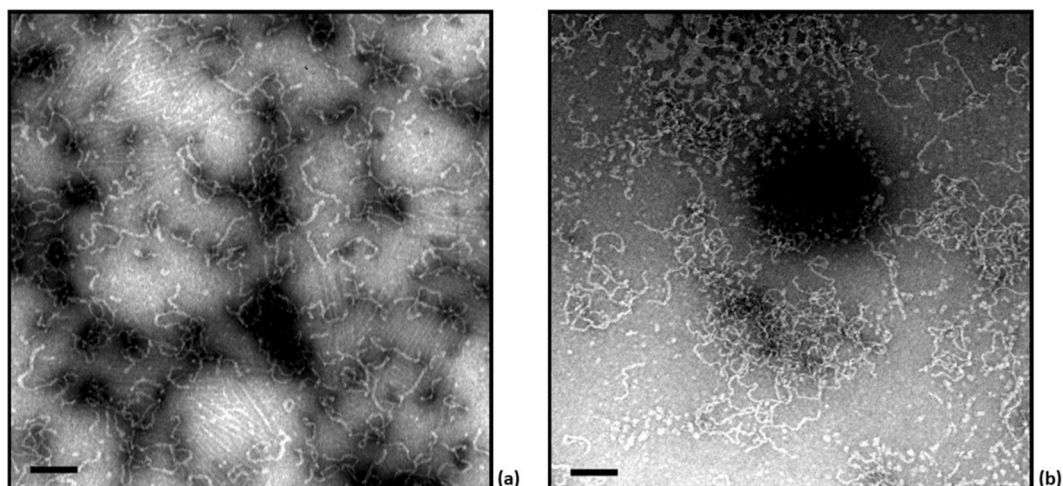

Fig. 5. Transmission electron micrographs (at 20,000× magnification) of 0,5 wt% ovalbumin solutions at pH 7 heated conventionally at 85 °C for 1200 s: heated (a) at low ionic strength, and (b) at high ionic strength. Scale bars represent 100 nm length.

anticipated aggregate clusters, as depicted in Fig. 5 (b). This reinforces the description by Weijers et al. [12], who characterized aggregate clusters as a consisting of fibrillar shaped-aggregates. Upon optical evaluation of the micrographs, no discernible differences in aggregate size were observed when comparing aggregates produced at different temperatures, HOLD or heating methods. Further, no substantial differences were apparent in aggregate size under low ionic strength and clusters size under high ionic strength. However, a range of aggregate size was visible in all samples. This includes smaller worm-like aggregates of approx. 20 nm, which appeared to be in an oligomeric state rather than mature AF, but also longer fibrillar-shaped aggregates with length up to approx. 250 nm. Cluster diameters ranged from approx. 200 to 500 nm. Comparable sizes of ovalbumin aggregates as well as cluster diameters were also reported via TEM by other authors [12].

3.6. Fourier-transform infrared spectroscopy

FTIR measurements of ovalbumin reveal distinct bands within the amide I band at wavelengths between 1600 and 1700 cm^{-1}, in agreement with other authors [48,49]. The obtained second derivate FTIR spectra of native ovalbumin exhibited prominent bands at approx. 1658, 1637, and 1624 cm^{-1}, indicative of alpha-helical and low-frequency (lf) beta-sheet structures. Further, bands at 1684 and 1673 as well as a band at 1646 cm^{-1} were associated to beta-turn and random coil structures, respectively. Irrespective of the type of treatment, all heated samples exhibited characteristics linked to a denatured or aggregated form of ovalbumin. This includes a reduction of alpha-helical and random coil structures, accompanied by an increase in beta-sheet and beta-turn structures. Notably, the beta-sheet band at 1636 cm^{-1} largely diminished, while a sharp rise at approx. 1622 cm^{-1} as well as an emerging high-frequency (hf) beta-sheet band at approx. 1693 cm^{-1} became evident, as shown in Fig. 6a. Comparable results are also described by Abrisomova et al. [49] or Milošević et al. [50], . The latter authors describe an increase in beta-sheet bands at 1624 and 1695 cm^{-1} to result from aggregation-specific beta-sheets, which are characteristic of FTIR spectra of AF forms. Thus, the ensuing discussion focusses on beta-sheet structures. Relative amounts of the analysed secondary protein structures of ovalbumin are outlined in Table 2.

In terms of relative quantities of beta-sheet structures, HOLD emerges as the most impactful factor, with samples at long HOLD consistently exhibiting higher values compared to those treated with short HOLD (as depicted in Fig. 6 (b)). When comparing the influence of final temperatures, differences in beta-sheet structures are noticeable for OH treated samples at short HOLD (as depicted in Fig. 6 (c)) but become less apparent or disappear at long HOLD or when treated via COV. This corresponds with our earlier results as MEF potentially impair the formation of beta-sheet and/or AF structures but show less influence when treatment time is prolonged.

Furthermore, mostly higher values for beta-sheet structures were observed in samples treated at high ionic strength compared to their counterparts treated at low ionic strength. This observation aligns with the results obtained from ThT measurement for both COV and OH treated samples at short HOLD, and is also described by Kato & Takagi [51]. The authors explain a higher amount of beta-sheet structures at high ionic strength with diminished repulsive forces between proteins and greater occurrence of intermolecular interactions, which we anticipate to occur under the conditions employed here. An increase in beta-sheet structures lead to heightened
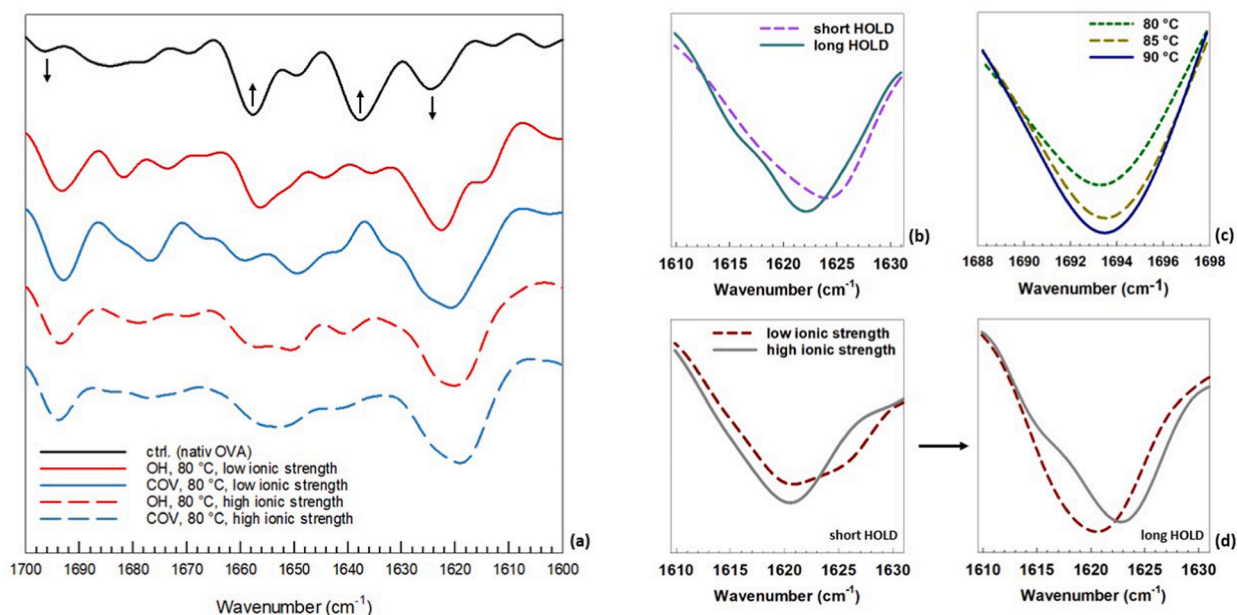

Fig. 6. Representative second derivate FTIR amide I region spectra of 0,5 wt% ovalbumin solutions heated under various conditions. (a) full amide I region spectra of proteins solutions heated at short holding time under conditions as indicated, ctrl. = untreated ovalbumin. (b) low-frequency beta-sheet region of conventionally heated samples at 85 °C at low ionic strength. (c) high-frequency beta-sheet region of ohmically heated samples at low ionic strength after short holding time (HOLD). (d) low-frequency beta sheet region of conventionally heated samples at 85 °C after short HOLD (left) and long HOLD (right).

Table 2
Relative amounts of secondary protein structures of 0,5 wt% ovalbumin at pH 7 heated under various conditions as indicated.

Ionic strength	HOLD	Heating Method	Alpha-helix (%) at 80 °C	at 85 °C	at 90 °C	Beta-sheet (%) at 80 °C	at 85 °C	at 90 °C	Beta-turn (%) at 80 °C	at 85 °C	at 90 °C	Random coil (%) at 80 °C	at 85 °C	at 90 °C
low	short	COV	20.7 ± 0.[c,d,A]	17.9 ± 1.0[c,d,B]	16.0 ± 0.4[c,C]	46.0 ± 0.7[d,A]	46.9 ± 1.1[c,A]	52.4 ± 0.3[c,B]	8.4 ± 1.9[b,c,d,A]	14.4 ± 0.5[d,B]	11.2 ± 1.1[e,C]	5.5 ± 0.7[a,c,A]	8.5 ± 1.4[e,B]	6.1 ± 0.2[e,A]
		OH	21.1 ± 0.6[c,d,A]	20.7 ± 0.7[d,A]	16.9 ± 0.1[d,B]	35.1 ± 1.9[b,A]	41.2 ± 0.5[b,B]	47.8 ± 0.6[b,C]	8.1 ± 1.2[b,c,d,A]	10.6 ± 1.6[c,A,B]	11.3 ± 0.7[e,B]	6.8 ± 0.3[e,A]	6.9 ± 1.1[d,e,A,B]	6.1 ± 0.2[e,B]
	long	COV	18.9 ± 1.2[b,A,B]	17.0 ± 1.2[b,c,A]	19.0 ± 0.5[e,B]	56.8 ± 1.2[f,A]	57.2 ± 0.8[e,A]	60.7 ± 1.4[e,B]	8.3 ± 1.0[b,d,A]	11.3 ± 1.3[c,B]	8.1 ± 0.2[c,A]	4.5 ± 0.6[b,c,A]	5.4 ± 0.9[a,b,c,d,A,B]	5.4 ± 0.1[c,B]
		OH	20.4 ± 0.5[b,c,A]	16.6 ± 0.2[b,B]	18.9 ± 0.2[e,A]	52.8 ± 1.4[e,A]	52.5 ± 0.9[d,A]	58.2 ± 0.8[d,B]	9.6 ± 1.3[d,A]	13.7 ± 1.8[c,d,B]	9.3 ± 0.5[d,A]	6.0 ± 0.7[a,e,A]	5.8 ± 1.0[a,b,c,d,A]	5.5 ± 0.8[a,b,c,A]
high	short	COV	22.3 ± 1.8[d,e,A]	20.6 ± 0.3[d,A]	12.2 ± 0.3[b,B]	49.4 ± 3.4[d,e,A]	48.6 ± 0.9[c,A]	60.7 ± 0.6[e,B]	6.6 ± 1.5[a,b,c,A]	7.8 ± 0.8[b,A]	8.1 ± 1.2[b,c,d,A]	4.8 ± 0.5[c,A,B]	5.5 ± 0.2[a,c,B]	4.4 ± 0.7[b,A]
		OH	22.3 ± 0.4[e,A]	21.7 ± 0.4[e,A]	16.0 ± 0.5[c,B]	42.0 ± 0.9[c,A]	48.2 ± 0.3[c,B]	58.2 ± 0.5[d,C]	7.2 ± 0.6[b,c,A]	8.2 ± 0.8[b,A,B]	8.4 ± 0.5[c,B]	6.6 ± 0.4[a,e,A]	5.3 ± 0.5[a,b,d,B]	4.6 ± 0.4[b,B]
	long	COV	17.6 ± 0.6[b,A]	19.6 ± 0.5[d,B]	19.2 ± 0.8[e,B]	60.7 ± 0.4[g,A]	63.0 ± 0.4[g,B]	67.9 ± 1.7[f,C]	7.1 ± 0.2[b,A]	8.2 ± 0.7[b,B]	11.3 ± 0.3[e,C]	3.7 ± 0.5[b,A]	4.2 ± 0.6[b,A]	5.6 ± 0.4[a,c,B]
		OH	21.0 ± 0.4[c,A]	20.1 ± 0.9[d,A]	17.9 ± 1.1[d,e,B]	59.3 ± 1.0[g,A]	59.8 ± 0.5[f,A]	58.2 ± 0.5[d,A]	7.7 ± 0.3[c,A]	7.8 ± 0.5[b,A]	6.7 ± 1.0[a,b,A]	4.6 ± 0.2[c,A]	4.7 ± 0.3[b,A]	4.4 ± 0.4[b,A]
ctrl. (nativ OVA)			28.1 ± 1.1[a]			39.0 ± 0.8[a]			5.0 ± 0.7[a]			6.5 ± 0.9[a,e]		

Different small superscripts indicate significant differences (P < 0,05) of values within each column.
Different capital superscripts indicate significant differences (P < 0,05) of values within each row for every secondary protein structure (e.g. alpha-helix).
HOLD = holding time, OH = Ohmic heating, COV = conventional heating.

ThT fluorescence, a rational outcome given that AF are composed of highly ordered beta-sheet structures. Similar findings are also described by Monge-Morera et al. [16] for ovalbumin and EWP. However, our results also reveal a change in peak height for lf beta-sheet structures between low and high ionic strength when looking at the influence of HOLD, as shown in Fig. 6d. At short HOLD, samples treated at high ionic strength exhibit a dominance in the lf beta-sheet band compared to samples at low ionic strength. After approx. 20 min of thermal treatment, i.e., after long HOLD, this phenomena reverses, with samples treated at low ionic strength now exhibiting a dominance the lf beta-sheet band. This trend is more pronounced at 80 and 85 °C than at 90 °C. When examining ThT staining results as described in section 2.3.2, a comparable tendency is visible for OH samples or COV samples at 80 °C. Samples at low ionic strength display a comparable or lower ThT fluorescence signal within the first half of treatment time compared to their counterparts at high ionic strength. However, towards the end of HOLD, this pattern shifts and samples at low ionic strength exhibit higher ThT fluorescence. This further supports the assumption that the formation of ovalbumin aggregate clusters may impede the formation of beta-sheets, consequently hindering the growth of AF structures after long HOLD.

In terms of secondary structures in OH treated samples compared to their COV treated counterparts, OH commonly resulted in lower percental values of aggregation-specific beta-sheet structures. Concurrently, the amount of alpha-helical structures decreases less when treated via OH. Hence, OH rather led to less and/or an altered denaturation and aggregation as also reported by others for different proteins, like egg white, potato or whey proteins [21–23,25]. Noteworthy, these changes were more evident within FTIR spectra at the lf beta-sheet structures at 1624 cm^{-1} wavelength and were less pronounced or absent at hf beta-sheet structures at 1695 cm^{-1}.

4. Conclusion

This study assessed how OH influences the aggregation of ovalbumin and the formation of AF structures under various environmental conditions. The application of MEF during thermal treatment induced lower amounts of AF structures. FFF results indicated that OH treated samples produced smaller sized aggregates as well as smaller aggregate clusters. We conclude that MEF impair the growth of AF aggregates by altering the denaturation of proteins, resulting in a conformation less prone to aggregation, characterized by lower levels of aggregation-specific beta-sheets but higher levels of native alpha helices. Additionally, the oscillating motion of molecules and aggregates disrupts the formation of aggregates and aggregate clusters, thereby impending aggregate growth.

The effects of increased electrical field strength can be neglected at the here used electrical set-up, as higher field strengths did not demonstrate a remarkable impact on AF formation. However, we conclude that repulsive forces due to different ionic strengths play a substantial role in the occurrence of AF aggregates, whether as single aggregates or as aggregate clusters. Furthermore, an elevation of treatment temperature as well as a prolonged HOLD leads to an increased formation of AF, which is associated to a higher total energy input.

This study has demonstrated that OH can be used as a tool for intentionally fine-tuning ovalbumin aggregates and AF structures. Given that the formation of AF is reducing during thermal treatment under OH, protein functionality may also be diminished. This can be of interest, for instance, in cases when lower gel strengths (e.g., for producing senior-friendly foods) or reduced foaming during a production process is desired. Moreover, OH can be employed as a heating technology that preserves more native protein structures, particularly when minimizing the impact on protein denaturation is a priority.

Future studies should address how the reduced amount of AF structures and aggregate size behave in food matrices, such as protein-stabilized gels, foams, or emulsions. Additionally, a closer examination of the AF structure is recommended to discern how MEF influence AF formation.

Funding statement

Data availability statement

The data associated with the present study has not been deposited into a publicly available repository. Data will be made available on request.

CRediT authorship contribution statement

Eike Joeres: Writing – original draft, Visualization, Investigation, Formal analysis, Data curation, Conceptualization. **Stephan Drusch:** Writing – review & editing, Supervision, Formal analysis. **Stefan Töpfl:** Writing – review & editing, Formal analysis. **Andreas Juadjur:** Writing – review & editing, Formal analysis. **Olympia Ekaterini Psathaki:** Writing – review & editing, Formal analysis, Data curation. **Volker Heinz:** Writing – review & editing, Formal analysis. **Nino Terjung:** Writing – review & editing, Supervision, Project administration, Conceptualization.

Declaration of competing interest

The authors declare that they have no known competing financial interests or personal relationships that could have appeared to influence the work reported in this paper.

Acknowledgement

Appendix A. Supplementary data

Supplementary data to this article can be found online at https://doi.org/10.1016/j.heliyon.2023.e22061.

References

[1] A. Goullieux, J.-P. Pain, in: Chapter 22 – Ohmic Heating, second ed., Elsevier Ltd, 2014 https://doi.org/10.1016/B978-0-12-411479-1.00022-X.

[2] P.J. Fellows, Dielectric, Ohmic and Infrared Heating, 2017, https://doi.org/10.1016/b978-0-08-100522-4.00019-5.

[3] R.M. Rodrigues, Z. Avelar, L. Machado, R.N. Pereira, A.A. Vicente, Electric field effects on proteins – novel perspectives on food and potential health implications, Food Res. Int. 137 (2020), https://doi.org/10.1016/j.foodres.2020.109709.

[4] H. Jaeger, A. Roth, S. Toepfl, T. Holzhauser, K.H. Engel, D. Knorr, R.F. Vogel, N. Bandick, S. Kulling, V. Heinz, P. Steinberg, Opinion on the use of ohmic heating for the treatment of foods, Trends Food Sci. Technol. 55 (2016) 84–97, https://doi.org/10.1016/j.tifs.2016.07.007.

[5] R.M. Rodrigues, R.N. Pereira, A.A. Vicente, A. Cavaco-Paulo, A. Ribeiro, Ohmic heating as a new tool for protein scaffold engineering, Mater. Sci. Eng. C. 120 (2021), https://doi.org/10.1016/j.msec.2020.111784.

[6] E.A. Foegeding, J.P. Davis, Food protein functionality: a comprehensive approach, Food Hydrocolloids 25 (2011) 1853–1864, https://doi.org/10.1016/j.foodhyd.2011.05.008.

[7] H.B. Wijayanti, A. Brodkorb, S.A. Hogan, E.G. Murphy, Thermal Denaturation, Aggregation, and Methods of Prevention, Elsevier Inc., 2018, https://doi.org/10.1016/B978-0-12-812124-5.00006-0.

[8] T. Nicolai, D. Durand, Controlled food protein aggregation for new functionality, Curr. Opin. Colloid Interface Sci. 18 (2013) 249–256, https://doi.org/10.1016/j.cocis.2013.03.001.

[9] T. Nicolai, Gelation of food protein-protein mixtures, Adv. Colloid Interface Sci. 270 (2019) 147–164, https://doi.org/10.1016/j.cis.2019.06.006.

[10] C. Lara, S. Gourdin-Bertin, J. Adamcik, S. Bolisetty, R. Mezzenga, Self-assembly of ovalbumin into amyloid and non-amyloid fibrils, Biomacromolecules 13 (2012) 4213–4221, https://doi.org/10.1021/bm301481v.

[11] M. Pouzot, T. Nicolai, R.W. Visschers, M. Weijers, X-ray and light scattering study of the structure of large protein aggregates at neutral pH, Food Hydrocolloids 19 (2005) 231–238, https://doi.org/10.1016/j.foodhyd.2004.06.003.

[12] M. Weijers, L.M.C. Sagis, C. Veerman, B. Sperber, E. Van Der Linden, Rheology and structure of ovalbumin gels at low pH and low ionic strength, Food Hydrocolloids 16 (2002) 269–276, https://doi.org/10.1016/S0268-005X(01)00097-2.

[13] Y. Meng, Z. Wei, C. Xue, Protein fibrils from different food sources: a review of fibrillation conditions, properties, applications and research trends, Trends Food Sci. Technol. 121 (2022) 59–75, https://doi.org/10.1016/j.tifs.2022.01.031.

[14] H. Khalesi, C. Sun, J. He, W. Lu, Y. Fang, The role of amyloid fibrils in the modification of whey protein isolate gels with the form of stranded and particulate microstructures, Food Res. Int. 140 (2021) 109856, https://doi.org/10.1016/j.foodres.2020.109856.

[15] T.P. Knowles, A.W. Fitzpatrick, S. Meehan, H.R. Mott, M. Vendruscolo, C.M. Dobson, M.E. Welland, Role of intermolecular forces in defining material properties of protein nanofibrils, Science 318 (2007) 1900–1903, https://doi.org/10.1126/science.1150057.

[16] M. Monge-Morera, M.A. Lambrecht, L.J. Deleu, G. Gallardo, N.N. Louros, M. De Vleeschouwer, F. Rousseau, J. Schymkowitz, J.A. Delcour, Processing induced changes in food proteins: amyloid formation during boiling of hen egg white, Biomacromolecules 21 (2020) 2218–2228, https://doi.org/10.1021/acs.biomac.0c00186.

[17] K.J.A. Jansens, I. Rombouts, C. Grootaert, K. Brijs, J. Van Camp, P. Van der Meeren, F. Rousseau, J. Schymkowitz, J.A. Delcour, Rational design of amyloid-like fibrillary structures for tailoring food protein techno-functionality and their potential health implications, Compr. Rev. Food Sci. Food Saf. 18 (2019) 84–105, https://doi.org/10.1111/1541-4337.12404.

[18] Y. Cao, R. Mezzenga, Food protein amyloid fibrils: origin, structure, formation, characterization, applications and health implications, Adv. Colloid Interface Sci. 269 (2019) 334–356, https://doi.org/10.1016/j.cis.2019.05.002.

[19] R.M. Rodrigues, A.A. Vicente, S.B. Petersen, R.N. Pereira, Electric field effects on β-lactoglobulin thermal unfolding as a function of pH – impact on protein functionality, Innov. Food Sci. Emerg. Technol. 52 (2019) 1–7, https://doi.org/10.1016/j.ifset.2018.11.010.

[20] C.P. Samaranayake, S.K. Sastry, In-situ activity of α-amylase in the presence of controlled-frequency moderate electric fields, LWT - Food Sci. Technol. 90 (2018) 448–454, https://doi.org/10.1016/j.lwt.2017.12.053.

[21] E. Joeres, S. Drusch, S. Töpfl, J. Auadjur, U. Bindrich, T. Völker, V. Heinz, N. Terjung, Ohmic vs. conventional heating: influence of moderate electric fields on properties of potato protein isolate gels, Innov. Food Sci. Emerg. Technol. 85 (2023), 103333, https://doi.org/10.1016/j.ifset.2023.103333.

[22] R.N. Pereira, J.A. Teixeira, A.A. Vicente, Exploring the denaturation of whey proteins upon application of moderate electric fields: a kinetic and thermodynamic study, J. Agric. Food Chem. 59 (2011) 11589–11597, https://doi.org/10.1021/jf201727s.

[23] R.M. Rodrigues, A.J. Martins, O.L. Ramos, F.X. Malcata, J.A. Teixeira, A.A. Vicente, R.N. Pereira, Influence of moderate electric fields on gelation of whey protein isolate, Food Hydrocolloids 43 (2015) 329–339, https://doi.org/10.1016/j.foodhyd.2014.06.002.

[24] Y. Chen, T. Wang, Y. Zhang, X. Yang, J. Du, D. Yu, F. Xie, Effect of moderate electric fields on the structural and gelation properties of pea protein isolate, Innov. Food Sci. Emerg. Technol. 77 (2022), 102959, https://doi.org/10.1016/j.ifset.2022.102959.

[25] E. Joeres, H. Schölzel, S. Drusch, S. Töpfl, V. Heinz, N. Terjung, Ohmic vs. conventional heating: influence of moderate electric fields on properties of egg white protein gels, Food Hydrocolloids 127 (2022), https://doi.org/10.1016/j.foodhyd.2022.107519.

[26] F. Schottroff, D. Biebl, M. Gruber, N. Burghardt, J. Schelling, M. Gratz, C. Schoenher, H. Jaeger, Inactivation of vegetative microorganisms by ohmic heating in the kilohertz range – evaluation of experimental setups and non-thermal effects, Innov. Food Sci. Emerg. Technol. 63 (2020), https://doi.org/10.1016/j.ifset.2020.102372.

[27] R.N. Pereira, R.M. Rodrigues, Ó.L. Ramos, F. Xavier Malcata, J.A. Teixeira, A.A. Vicente, Production of whey protein-based aggregates under ohmic heating, Food Bioprocess Technol. 9 (2016) 576–587, https://doi.org/10.1007/s11947-015-1651-4.

[28] J. Jurgelevičiūtė, N. Bičkovas, A. Sakalauskas, V. Novickij, V. Smirnovas, E. Lastauskienė, Effects of pulsed electric fields on yeast with prions and the structure of amyloid fibrils, Appl. Sci. 11 (2021) 1–10, https://doi.org/10.3390/app11062684.

[29] N.K. Pandey, S. Mitra, S. Chakraborty, S. Ghosh, S. Sen, S. Dasgupta, S. DasGupta, Disruption of human serum albumin fibrils by a static electric field, J. Phys. D Appl. Phys. 47 (2014), https://doi.org/10.1088/0022-3727/47/30/305401.

[30] C.A. Hettiarachchi, L.D. Melton, J.A. Gerrard, S.M. Loveday, Formation of β-lactoglobulin nanofibrils by microwave heating gives a peptide composition different from conventional heating, Biomacromolecules 13 (2012) 2868–2880, https://doi.org/10.1021/bm300896r.

[31] N. Todorova, A. Bentvelzen, I. Yarovsky, Electromagnetic field modulates aggregation propensity of amyloid peptides, J. Chem. Phys. 152 (2020), https://doi.org/10.1063/1.5126367.

[32] M. Lassé, D. Ulluwishewa, J. Healy, D. Thompson, A. Miller, N. Roy, K. Chitcholtan, J.A. Gerrard, Evaluation of protease resistance and toxicity of amyloid-like food fibrils from whey, soy, kidney bean, and egg white, Food Chem. 192 (2016) 491–498, https://doi.org/10.1016/j.foodchem.2015.07.044.

[33] F.G. Pearce, S.H. Mackintosh, J.A. Gerrard, Formation of amyloid-like fibrils by ovalbumin and related proteins under conditions relevant to food processing, J. Agric. Food Chem. 55 (2007) 318–322, https://doi.org/10.1021/jf062154p.

[34] L. Josefsson, X. Ye, C.J. Brett, J. Meijer, C. Olsson, A. Sjögren, J. Sundlöf, A. Davydok, M. Langton, Å. Emmer, C. Lendel, Potato protein nanofibrils produced from a starch industry sidestream, ACS Sustain. Chem. Eng. 8 (2020) 1058–1067, https://doi.org/10.1021/acssuschemeng.9b05865.

[35] H. Kieserling, A. Pankow, J.K. Keppler, A.M. Wagemans, S. Drusch, Conformational state and charge determine the interfacial film formation and film stability of β-lactoglobulin, Food Hydrocolloids 114 (2021), https://doi.org/10.1016/j.foodhyd.2020.106561.

[36] M. Pero, H. Kiani, G. Askari, A novel numerical approach for modeling the coagulation phenomenon in egg white, J. Food Process. Eng. 42 (2019) 1–11, https://doi.org/10.1111/jfpe.13033.

[37] K. Iwashita, N. Inoue, A. Handa, K. Shiraki, Thermal aggregation of hen egg white proteins in the presence of salts, Protein J. 34 (2015) 212–219, https://doi.org/10.1007/s10930-015-9612-3.

[38] M.R. Nilsson, Techniques to study amyloid fibril formation in vitro, Methods 34 (2004) 151–160, https://doi.org/10.1016/j.ymeth.2004.03.012.

[39] W.E. Klunk, R.F. Jacob, R.P. Mason, Quantifying amyloid by Congo red spectral shift assay, Methods Enzymol. 309 (1999) 285–305, https://doi.org/10.1016/S0076-6879(99)09021-7.

[40] R. Eisert, L. Felau, L.R. Brown, Methods for enhancing the accuracy and reproducibility of Congo red and thioflavin T assays, Anal. Biochem. 353 (2006) 144–146, https://doi.org/10.1016/j.ab.2006.03.015.

[41] A. Espargaró, S. Llabrés, S.J. Saupe, C. Curutchet, F.J. Luque, R. Sabaté, On the binding of Congo red to amyloid fibrils, Angew. Chemie - Int. Ed. 59 (2020) 8104–8107, https://doi.org/10.1002/anie.201916630.

[42] M. Ferreira, C. Hofer, A. Raemy, A calorimetric study of egg white proteins, J. Therm. Anal. 48 (1997) 683–690, https://doi.org/10.1007/BF01979514.

[43] Y. Wang, Y. Shen, G. Qi, Y. Li, X.S. Sun, D. Qiu, Y. Li, Formation and physicochemical properties of amyloid fibrils from soy protein, Int. J. Biol. Macromol. 149 (2020) 609–616, https://doi.org/10.1016/j.ijbiomac.2020.01.258.

[44] R.M. Rodrigues, L.H. Fasolin, Z. Avelar, S.B. Petersen, A.A. Vicente, R.N. Pereira, Effects of moderate electric fields on cold-set gelation of whey proteins – from molecular interactions to functional properties, Food Hydrocolloids 101 (2020), https://doi.org/10.1016/j.foodhyd.2019.105505.

[45] M. Weijers, R.W. Visschers, T. Nicolai, Light scattering study of heat-induced aggregation and gelation of ovalbumin, Macromolecules 35 (2002) 4753–4762, https://doi.org/10.1021/ma0120198.

[46] T. Koseki, T. Fukuda, N. Kitabatake, E. Doi, Characterization of linear polymers induced by thermal denaturation of ovalbumin, Top. Catal. 3 (1989) 135–148, https://doi.org/10.1016/S0268-005X(89)80023-2.

[47] R.N. Pereira, R.M. Rodrigues, E. Altinok, Ó.L. Ramos, F. Xavier Malcata, P. Maresca, G. Ferrari, J.A. Teixeira, A.A. Vicente, Development of iron-rich whey protein hydrogels following application of ohmic heating – effects of moderate electric fields, Food Res. Int. 99 (2017) 435–443, https://doi.org/10.1016/j.foodres.2017.05.023.

[48] J. Milošević, B. Jovčić, B. Janković, N. Polović, Exploring the potential of infrared spectroscopy in qualitative and quantitative monitoring of ovalbumin amyloid fibrillation, Spectrochim. Acta Part A Mol. Biomol. Spectrosc. 229 (2020) 117882, https://doi.org/10.1016/j.saa.2019.117882.

[49] K.V. Abrosimova, O.V. Shulenina, S.V. Paston, FTIR study of secondary structure of bovine serum albumin and ovalbumin, J. Phys. Conf. Ser. 769 (2016), https://doi.org/10.1088/1742-6596/769/1/012016.

[50] J. Milošević, R. Prodanović, N. Polović, On the protein fibrillation pathway: oligomer intermediates detection using ATR-FTIR spectroscopy, Molecules 26 (2021), https://doi.org/10.3390/molecules26040970.

[51] A. Kato, T. Takagi, Formation of intermolecular β-sheet structure during heat denaturation of ovalbumin, J. Agric. Food Chem. 36 (1988) 1156–1159, https://doi.org/10.1021/jf00084a007.